Bull. Nov. Comp. Center, Math. Model. in Geoph., 5 (1999), 25–40
© 1999 NCC Publisher

Numerical solution to combined one-dimensional inverse problems for Maxwell's equation and equations of porous media*

E.V. Goryunov, Kh.Kh. Imomnazarov

Combined one-dimensional inverse problems for Maxwell's equation and equations of porous media are solved numerically using the optimization approach. Representative series of numerical calculations for various models of media are given.

Introduction

The choice of simplifying assumptions on a real geological medium is especially important in the interpretation of geophysical data. As a rule, the geological medium is assumed ideally elastic in most cases. Real geological media, however, are multiphase, conducting, fracturous, porous, etc. During the propagation of seismic waves their dissipation which is associated with energy absorption takes place.

The numerical solution of some combined one-dimensional inverse problems for the equations of SH waves in conducting porous media using the optimization approach is considered. Theoretical aspects of some combined one-dimensional inverse problems can be found in [1–4] and their references.

1. Numerical determination of conductivity of porous body, liquid, density of conductivity of the porous body

Assume that a half-space $z > 0$ is filled with a conducting porous medium with the parameters λ, μ, α, the conductivities σ_l, σ_s and the partial densities $\rho_{0,l}$, $\rho_{0,s}$ which are functions of the coordinates x, y, z. In the case of a one-dimensional inhomogeneous medium, the process of propagation of SH waves is described by the following initial boundary value problem [5]:

*Supported by the Russian Foundation for Basic Research under Grant 99-05-64538 and the Youth Grant of the Siberian Branch of the Russian Academy of Sciences.

$$\rho_{0,s}(z)u_{tt} - (\mu u_z)_z = 0, \quad t \in R, \quad z > 0, \tag{1}$$

$$\sigma(z)E_t - E_{zz} + H\sigma_s(z)u_t = 0, \quad t \in R, \quad z > 0, \tag{2}$$

$$u|_{t<0} = 0, \quad z > 0, \tag{3}$$

$$E|_{t<0} = 0, \quad z > 0, \tag{4}$$

$$\mu u_z|_{z=0} = f(t), \quad t \in R_1 \tag{5}$$

$$E_z|_{z=0} = 0, \quad t \in R_1. \tag{6}$$

Here $u(t,z)$ and $E(t,z)$ are the horizontal components of the displacement vector of the velocity of particles of the conducting elastic porous body and the electric field, respectively [5], $f(t)$ is the form of a sounding signal (a finite continuously differentiable function on the interval $[0,\infty)$), $\mu = \text{const}$ is the shear modulus, $\rho_{0,s}(z)$ is the partial density of the elastic porous body, $\sigma(z) = \sigma_l(z) + \sigma_s(z)$, $\sigma_s(z)$, and $\sigma_l(z)$ are conductivities of the body and the liquid, respectively [3].

In paper [6], it was found that for the conducting porous media the Archie law holds: $\sigma_l/\sigma = \rho_{0,l}^m$ (the consolidation index m is designed from the empirical grounds and it varies for different rocks within (1.3, 3) [7], we assume $m = 1.3$ in the sequel).

In this case, partial density of the elastic porous body $\rho_{0,s}(z)$ and liquid $\rho_{0,l}(z)$ are connected with the physical densities of the elastic porous body $\rho_s^f(z)$ and the liquid $\rho_l^f(z)$ by the formulas $\rho_{0,s}(z) = \rho_s^f(z)\,(1-d(z))$, $\rho_{0,l}(z) = \rho_l^f(z)\,d(z)$, where $d(z)$ is porosity.

The determination of $u(t,z)$ and $E(t,z)$ from (1)–(6), given the function $\rho_s^f(z)$, $d(z)$, $\sigma_l(z)$, $\sigma_s(z)$ from $\mathcal{M} = \{m(z) \mid 0 < \delta \le m(z) \le \Delta < \infty,\ \lim_{z\to\infty} m(z) = m_0,\ m(z) - m_0 \in L_2(0,\infty) \cap C^1(0,\infty)\}$ is the direct problem, and the determination of the functions $\rho_s^f(z)$, $\sigma_l(z)$, $\sigma_s(z)$ ($d(z)$ and H are assumed to be known) using the complementary information

$$u|_{z=0} = u_0(t), \quad t \in R_1, \tag{7}$$

$$E|_{z=0} = E_0(t), \quad t \in R_1, \tag{8}$$

is the inverse problem for the system of equations of SH waves in the conducting porous medium.

We seek for the solution to the combined inverse problem as a minimum point of the misfit functionals

$$\Phi_1[\rho_s^f(z)] = \int_0^\infty |u_0(t) - B_1[\rho_s^f(z)](t)|^2 dt, \tag{9}$$

$$\Phi_2[\sigma(z)] = \int_0^\infty |E_0(t) - B_2[\sigma(z)](t)|^2 dt. \tag{10}$$

Here $B_1[\rho_s^f(z)](t)$ and $B_2[\sigma(z)](t)$ are operators that transform the functions $\rho_s^f(z)$ and $\sigma(z)$ into the solutions to the initial boundary value problems (1)–(8) at $z = 0$:

$$B_1[\rho_s^f(z)](t) = u_0(t), \quad B_2[\sigma(z)](t) = E_0(t)\,.$$

The issues connected with the uniqueness of a minimum point of the misfit functional (9) and the existence of the gradient are considered in [8]. For misfit functional (10) the uniqueness of a minimum point and the existence of the gradient are similarly proved.

Since functionals (9) and (10) are quadratic, it is reasonable to realize the iterative process of the search for the minimum in the frequency domain using the Parseval equality. Thereby we avoid the labor-consuming operation of the transfer from the frequency domain to the time domain in the solution to the direct combined problem. It permits to make a considerable reduction of computations. In the frequency domain, functionals (9), (10) take the form

$$\Phi_1[\rho_s^f(z)] = \int_{\omega_1}^{\omega_2} |\hat{u}_0(\omega) - \hat{B}_1[\rho_s^f(z)](\omega)|^2 d\omega, \tag{11}$$

$$\Phi_2[\sigma(z)] = \int_{\omega_1}^{\omega_2} |\hat{E}_0(\omega) - \hat{B}_2[\sigma(z)](\omega)|^2 d\omega. \tag{12}$$

Here (ω_1, ω_2) is the range of the time frequencies determined by a composition of the sounding signal $F(\omega)$,

$$(\hat{u}_0(\omega), \hat{E}_0(\omega), F(\omega)) = \int_0^{\infty} (u_0(t), E_0(t)\rho_{0,s}(0)\, c_t^2(0) f(t)) \mathrm{e}^{-i\omega t} dt.$$

In terms of the Fourier transforms, $\hat{u}(\omega, z)$ and $\hat{E}(\omega, z)$ satisfy the following boundary value problem

$$\frac{d^2\hat{u}}{dz^2} + \omega^2 n_t^2(z)\,\hat{u} = 0, \quad z \in \Omega, \tag{13}$$

$$\frac{d^2\hat{E}}{dz^2} + i\omega\,\sigma(z)\,\hat{E} + i\omega H\,\sigma_s(z)\,\hat{u} = 0, \quad z \in \Omega, \tag{14}$$

$$\hat{u}_z|_{z=0} = F(\omega), \tag{15}$$

$$\hat{E}_z|_{z=0} = 0. \tag{16}$$

Here $n_t^2(z) = \rho_{0,s}(z)/\mu$. In formula (15), we use the definition of the transverse wave velocity $c_t(z) = \sqrt{\mu/\rho_{0,s}(z)}$.

As in [3, 9], it can be shown that the gradients of the misfit functionals (11) and (12) have the form

$$\nabla_{\rho_s^f(z)}\Phi_1[\rho_s^f(z)](s) = -\frac{2}{\mu}\mathrm{Re}\int_{\omega_1}^{\omega_2}\left[\hat{u}_0(\omega) - \hat{B}_1[\rho_s^f(z)](\omega)\right]\overline{G_t(s,\omega)}d\omega,$$

$$\nabla_{\sigma(z)}\Phi_2[\sigma(z)](s) = 2H\,\mathrm{Re}\int_{\omega_1}^{\omega_2}\omega^2\left[\hat{E}_0(\omega) - \hat{B}_2[\sigma(z)](\omega)\right]\overline{G_\sigma(s,\omega)}\,\overline{w(s,\omega)}d\omega +$$

$$2H\,\mathrm{Im}\int_{\omega_1}^{\omega_2}\omega^3\left[\hat{E}_0(\omega) - \hat{B}_2[\sigma(z)](\omega)\right]\overline{G_\sigma(s,\omega)}\times$$

$$\int_0^\infty \sigma(\tau)\overline{G_\sigma(\tau,\omega)w(\tau,\omega)}\,d\tau\,d\omega, \qquad (12')$$

$$w(\omega,z) = (1-\rho_{0,l}^{1,3}(z))\,u(\omega,z).$$

Here $G_s(z,\omega)$ is Green's function for the operator $\frac{d^2}{dz^2} - \omega^2 n_s^2(z)$, $n_\sigma^2(z) = -i\omega\sigma(z)$, a bar over the function denotes the complex conjugation.

2. Numerical determination of conductivity of porous body, liquid, and friction coefficient

The propagation of SH waves in the case of the energy dissipation caused by the friction coefficient $\chi(z)$, in a one-dimensional inhomogeneous medium is described by the initial boundary value problem (2), (4), (6) and

$$\rho_{0,s}(z)u_{tt} - (\mu u_z)_z + \chi(z)\rho_{0,l}^2(z)(u_t - v_t) = 0, \quad t \in R, \quad z > 0, \qquad (17)$$

$$v_{tt} - \chi(z)\rho_{0,l}(z)(u_t - v_t) = 0, \quad t \in R, \quad z > 0, \qquad (18)$$

$$u|_{t<0} = 0, \quad v|_{t<0} = 0, \quad z > 0. \qquad (19)$$

Here $v(t,z)$ is the horizontal velocity component of the conducting liquid with the partial density $\rho_{0,l}(z)$.

Inverse problem 1. *It is necessary to determine the functions $\sigma_l(z)$, $\sigma_l(z)$, $\chi(z) \in \mathcal{M}$ (given the functions $c_t(z)$, $\rho_{0,l}(z)$, $\rho_{0,s}(z) \in \mathcal{M}$ and constants H) from* (2), (4)–(8), (17)–(19).

We search for the solution to this combined inverse problem as a minimum point of the misfit functionals (10)

$$\Phi_3[\chi(z)] = \int_0^\infty |u_0(t) - B_3[\chi(z)](t)|^2 dt. \qquad (20)$$

Here $B_3[\chi(z)](t)$ is the operator that transforms the function $\chi(z)$ into the solutions to the initial boundary value problems (5), (17)–(19) at $z = 0$.

Passing into the frequency domain, after simple transformations we obtain, for $\hat{u}(\omega,z)$, the following boundary value problem (15):

$$\frac{d^2\hat{u}}{dz^2} + \left(1 + i\frac{\rho_{0,l}^2(z)}{\rho_{0,s}(z)}\frac{\chi(z)}{\omega + i\chi(z)\rho_{0,l}(z)}\right)\omega^2 n_i^2(z)\hat{u} = 0, \quad z \in \Omega.$$

In this case, the function $\hat{v}(\omega, z)$ is determined by the formula

$$\hat{v} = i\frac{\chi(z)\rho_{0,l}(z)}{\omega + i\chi(z)\rho_{0,l}(z)}\hat{u}.$$

Functional (20) and its gradient in the frequency domain have the form

$$\Phi_3[\chi(z)] = \int_{\omega_1}^{\omega_2} |\hat{u}_0(\omega) - \hat{B}_3[\chi(z)](\omega)|^2 d\omega,$$

$$\nabla_{\chi(z)}\Phi_3[\chi(z)](s) = -2\frac{\rho_{0,l}^2(s)}{\rho_{0,s}^2(s)}\mathrm{Re}\int_{\omega_1}^{\omega_2}\frac{\omega^3}{(\omega - i\,\chi\,\rho_{0,l}(s))^2} \times \left[\hat{u}_0(\omega) - \hat{B}_3[\chi(z)](\omega)\right]\overline{G}_\chi(s,\omega)\,d\omega.$$

Here $G_\chi(s,\omega)$ is Green's function of problem (5), (17)–(19).

Remark. The case of magnetic fields is considered in a similar way.

3. Numerical experiments

A program package in C++ with an extended graphic interface was written for the numerical experiments. It made it possible to reconstruct the functions $c_t(z)$, $\sigma_l(z)$, $\sigma_s(z)$.

To organize the iterative process of search for the minimum points of the misfit functionals, we used the method of conjugate gradients in the following interpretation:

$$\begin{aligned} f_{j+1}(z) &= f_j(z) - \alpha_j P_j(z), \\ \alpha_j &= \arg\min_{a\geq 0}\Phi[f_j(z) - \alpha P_j(z)], \\ P_0(z) &= \nabla_f\Phi[f_0(z)], \\ P_j(z) &= \nabla_f\Phi[f_j(z)] - \beta_j P_j(z), \quad j \geq 1, \\ \beta_j &= \left(\nabla_f\Phi[f_j(z)], \nabla_f\Phi[f_{j-1}(z)] - \nabla_f\Phi[f_j(z)]\right), \end{aligned}$$

where $f(z)$ and $\Phi[f(z)]$ take the values $c_t(z)$, $\sigma(z)$, $\chi(z)$ and $\Phi[c_t(z)]$, $\Phi[\sigma(z)]$, $\Phi[\chi(z)]$, and the step α_j is chosen using the "golden section" method.

As a sounding signal, we chose a pulse with the "bell-shaped envelope" with the dominant frequency $f = 20$ Hz (Figure 1):

$$F(\omega) = \left[\exp\left(-\left(\frac{\omega - 2\pi f}{\pi f}\right)^2\right) + \exp\left(-\left(\frac{\omega + 2\pi f}{\pi f}\right)^2\right)\right] \exp\left(-i\frac{1.75\omega}{f}\right).$$

The calculations were made for the time frequency of range 2–40 Hz.

A simple model was chosen in the first case: 4 layers of equal thickness located on underlying half-space (the distribution of the basic porosity is presented in Figure 2). All the models that the physical density of the liquid was assumed equal to 1 g/cm^3.

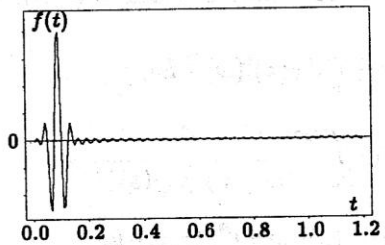

Figure 1

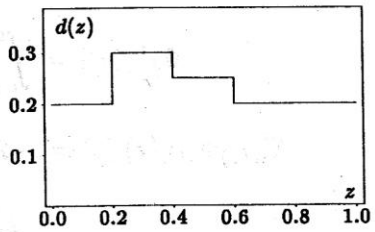

Figure 2

It is also necessary to add the sewing conditions at the interfaces of layers:

$$[\hat{u}]|_{z=z_k} = [\hat{u}_z]|_{z=z_k} = 0, \quad [\hat{E}]|_{z=z_k} = [\sigma^{-1}\hat{E}_z]|_{z=z_k} = 0.$$

The initial velocity approximation $c_{t0}(z)$ shown in Figure 3 with a dashed line was chosen in the form of a linear function not containing any information about waveguides and high-speed layers. The initial approximation for

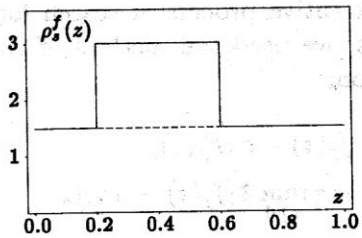

Figure 3

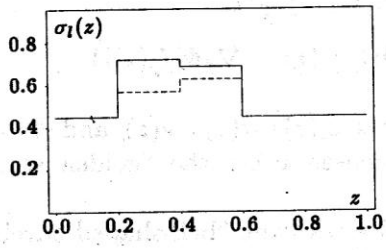

Figure 4

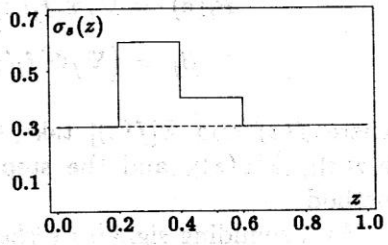

Figure 5

the conductivity of the liquid and porous elastic body are shown in Figures 4 and 5, respectively.

The wave field and the electric field intensities on the surface are presented in Figure 6 ($u(t,z)|_{z=0}$) and Figure 7 ($E(t,z)|_{z=0}$), respectively. It is seen from the figures that the measured fields and the fields calculated for the initial approximation substantially differ.

The corresponding full wave field and the electric field intensities are presented in Figures 8 and 9.

The velocity $c_t(z)$ was reconstructed at the first stage. The obtained velocities are shown in Figure 10. The wave field $u(t,0)$ on the surface calculated for them is presented in Figure 11, and the electric field intensity $E(t,0)$ – in Figure 12. The wave shape for the wave field was reconstructed

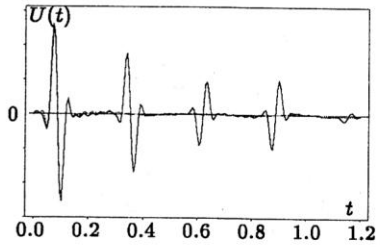

Figure 6

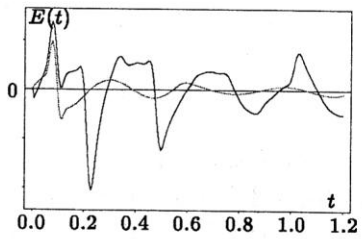

Figure 7

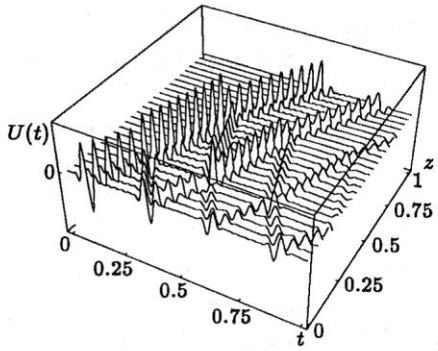

Figure 8

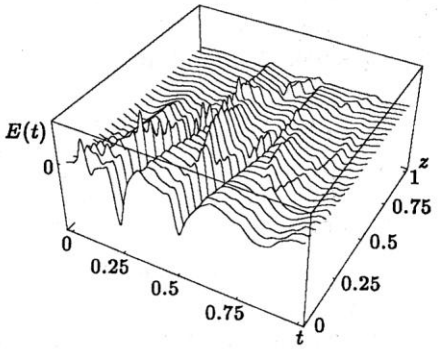

Figure 9

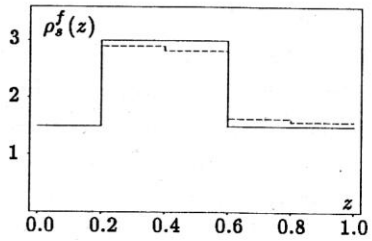

Figure 10

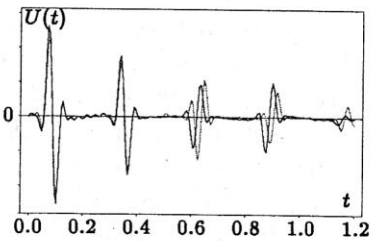

Figure 11

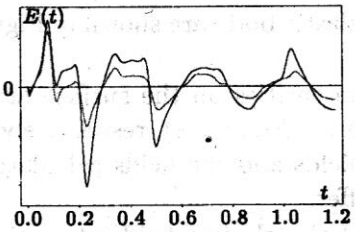

Figure 12

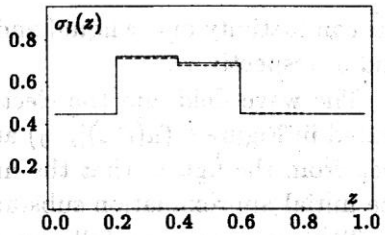

Figure 13

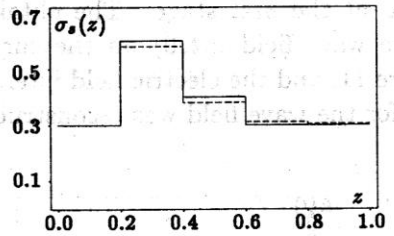

Figure 14

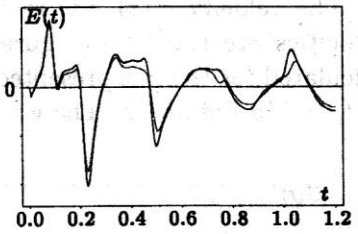

Figure 15

reasonably well, with the exception of a small phase lag, and for the electric field intensity, the general shape of the calculated signal differed from that of the recorded signal mainly in amplitude.

Then the conductivity of the medium $\sigma(z)$ was reconstructed. Using the Archie law and the determination of conductivity, the conductivities of the liquid (Figure 13) and the elastic porous body (Figure 14) were calculated. The electric field intensity on the surface calculated for them is shown in Figure 15.

A more complex model was chosen in the second case: 6 layers of equal thickness located on underlying half-space (the distribution of the basic porosity is shown in Figure 16).

The velocity distribution for this model (Figure 17) had a screened waveguide. This made difficult the reconstruction of the structure characteristics of the medium. The reconstruction of the distributions of the conductivities of the liquid (Figure 18) and the elastic porous body (Figure 19) was also not easy.

The calculated wave field and the electric field intensity on the surface are presented in Figures 20 and 21, respectively.

As for the first model, the distribution of the velocity $c_t(z)$ was reconstructed at the first stage. The velocity distribution obtained is shown in Figure 22. The wave field $u(t,0)$ on the surface calculated for it is presented in Figure 23, and the electric field intensity $E(t,0)$ in Figure 24.

Then the conductivity of the medium was reconstructed. The results obtained for the conductivity of the liquid, the elastic porous body, and the electric field intensity on the surface are presented in Figures 25, 26, and 27.

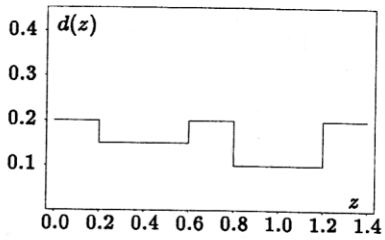

Figure 16

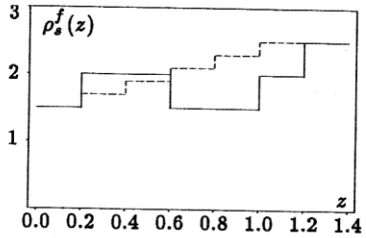

Figure 17

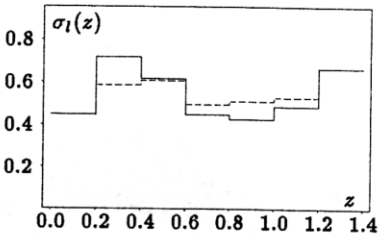

Figure 18

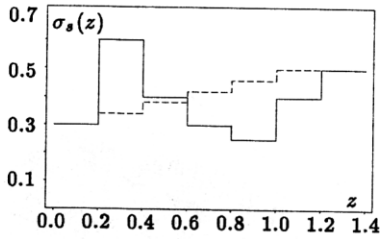

Figure 19

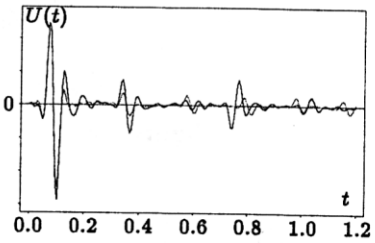

Figure 20

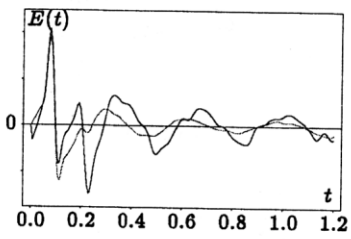

Figure 21

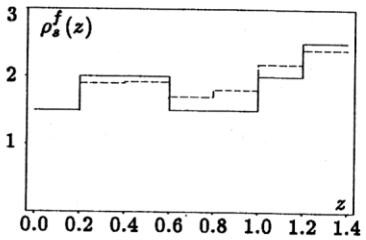

Figure 22

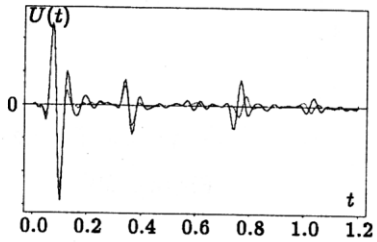

Figure 23

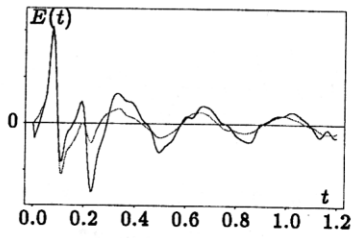

Figure 24

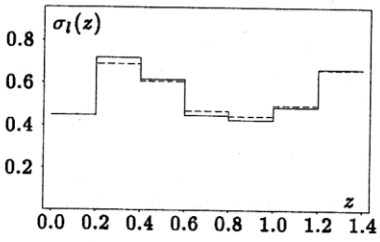

Figure 25

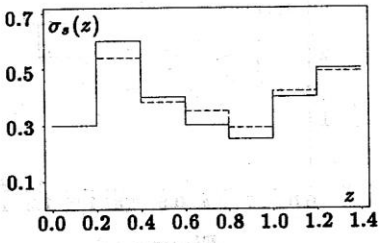

Figure 26

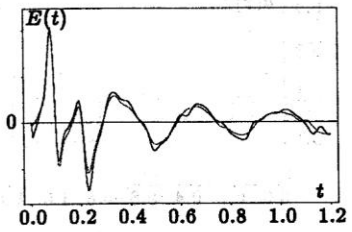

Figure 27

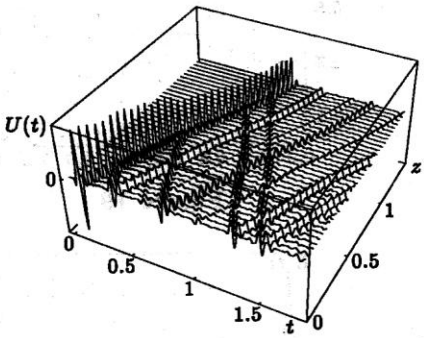

Figure 28

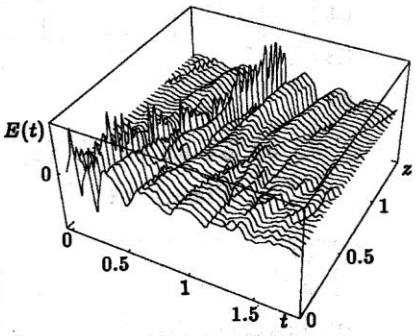

Figure 29

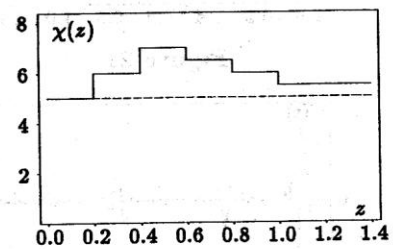

Figure 30

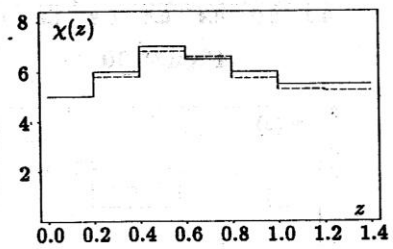

Figure 31

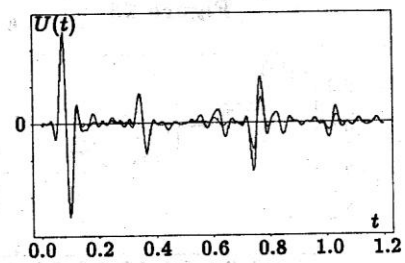

Figure 32

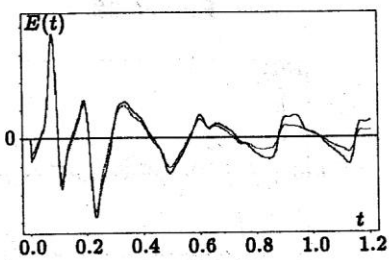

Figure 33

In the third case, the friction coefficient $\chi(z)$ with the basic parameters of the medium for the second model was reconstructed. The full wave fields for this model are presented in Figures 28 and 29.

The distribution of the friction coefficient is presented in Figure 30, and its reconstructed value – in Figure 31.

The wave field and the electric field intensities on the surface for the second model (solid line) and the third model with the introduced friction coefficient (dashed line) are given in Figures 32 and 33 for comparison. It can be seen that the allowance for the friction coefficient causes the amplitude decay of the incoming signal, i.e., energy dissipation, which logically follows from the physical picture of the phenomenon.

4. Numerical determination of conductivity of a porous elastic body, liquid, and second longitudinal wave velocity

Assume that vectors of velocity elements of the porous elastic body $\boldsymbol{u}(t,z)$ and the liquid $\boldsymbol{v}(t,z)$ are directed along the axis z, i.e., $\boldsymbol{u}(t,z) = (0,0,u(t,z))$, $\boldsymbol{v}(t,z) = (0,0,v(t,z))$. The electric field intensity $\boldsymbol{E}(t,z)$ is directed along the axis y, i.e., $\boldsymbol{E}(t,z) = (0,E(t,z),0)$.

In the case of a one-dimensional inhomogeneous medium, the process of propagation of seismic waves is described by the following initial boundary value problem [3, 5]:

$$u_{tt} - a_1(z)u_{zz} + a_2(z)v_{zz} = 0, \quad t \in R, \quad z > 0, \tag{21}$$

$$v_{tt} + a_3(z)u_{zz} - a_4(z)v_{zz} = 0, \quad t \in R, \quad z > 0, \tag{22}$$

$$\sigma(z)E_t - E_{zz} + H\sigma_s(z)u_t + H\sigma_l(z)\,v_t = 0, \quad t \in R, \quad z > 0, \tag{23}$$

$$(u,v)|_{t<0} = 0, \quad z > 0, \tag{24}$$

$$E|_{t<0} = 0, \quad z > 0, \tag{25}$$

$$(\tilde{h}_{33} + p)|_{z=0} = f(t), \quad \frac{\rho_{0,l}}{\rho_0} p|_{z=0} = 0, \quad t \in R_1, \tag{26}$$

$$E_z|_{z=0} = 0, \quad t \in R_1. \tag{27}$$

Here $f(t)$ is the form of a sounding signal (a finite continuously differentiable function on the interval $[0,\infty)$), $\rho_{0,s}(z)(\sigma_s(z))$ and $\rho_{0,l}(z)(\sigma_l(z))$ is the partial density of the porous elastic body and the liquid, respectively, $\sigma(z) = \sigma_l(z) + \sigma_s(z)$, $\rho_0(z) = \rho_{0,l}(z) + \rho_{0,s}(z)$, $\hat{h}_{ij}$ is the tensor of tension, p is pressure, the coefficients $a_n, n = \overline{1,4}$ are expressed by the velocities of longitude c_{l_m}, $m = 1,2$, transverse c_t waves, and by the ratio of the porous body and the liquid partial densities $\frac{\rho_{0,l}}{\rho_{0,s}}$ [10]:

$$a_1 = \frac{\rho_{0,l}}{\rho_0}\left(c_{l_1}^2 + c_{l_2}^2\right) + \frac{4}{3}\frac{\rho_{0,s}^2}{\rho_0^2}c_t^2 + \frac{\rho_{0,s}-\rho_{0,l}}{\rho_0}\tilde{z},$$

$$a_2 = \frac{\rho_{0,l}}{\rho_0}\left(c_{l_1}^2 + c_{l_2}^2 - 2\tilde{z} - \frac{4}{3}c_t^2\right),$$

$$a_3 = \frac{\rho_{0,s}}{\rho_0}\left(c_{l_1}^2 + c_{l_2}^2 - 2\tilde{z} - \frac{4}{3}c_t^2\right),$$

$$a_4 = \frac{\rho_{0,s}}{\rho_0}\left(c_{l_1}^2 + c_{l_2}^2 - \frac{4}{3}c_t^2\right) - \frac{\rho_{0,s}-\rho_{0,l}}{\rho_0}\tilde{z},$$

$$\tilde{z} = \frac{1}{2}\left(c_{l_1}^2 + c_{l_2}^2 - \frac{8}{3}\frac{\rho_{0,s}}{\rho_0}c_t^2\right) + \sqrt{\frac{1}{4}\left(c_{l_1}^2 - c_{l_2}^2\right)^2 - \frac{16}{9}\frac{\rho_{0,l}\rho_{0,s}}{\rho_0^2}c_t^4}.$$

Inverse problem 2 [1]. *Find the functions $\sigma_l(z), \sigma_s(z), c_{l_2}(z) \in \mathcal{M}$ (given the functions $c_t(z), c_{l_1}(z), \rho_{0,l}(z), \rho_{0,s}(z) \in \mathcal{M}$, $f(t)$, and constant H) from equations* (21)–(27) *through the complementary information*

$$u|_{z=0} = u_0(t), \quad t \in R_1, \tag{28}$$

$$E|_{z=0} = E_0(t), \quad t \in R_1. \tag{29}$$

We seek for the solution to the combined inverse problem as a minimum point of the misfit functionals

$$\Phi_1[c_{l_2}(z)] = \int_{\omega_1}^{\omega_2} |\hat{u}_0(\omega) - \hat{B}_1[c_{l_2}(z)](\omega)|^2\, d\omega, \tag{30}$$

$$\Phi_2[\sigma(z)] = \int_{\omega_1}^{\omega_2} |\hat{E}_0(\omega) - \hat{B}_2[\sigma(z)](\omega)|^2\, d\omega. \tag{31}$$

Here $\hat{B}_1[c_{l_2}(z)](\omega)$ and $\hat{B}_2[\sigma(z)](\omega)$ are operators which transform the functions $c_{l_2}(z)$, $F(\omega)$, and $\sigma(z)$ into the solutions to the initial boundary value problems (21)–(29) in a frequency domain at $z = 0$, (ω_1, ω_2) is the range of the time frequencies determined by composition of the sounding signal $F(\omega)$

$$(\hat{u}_0(\omega), \hat{E}_0(\omega), F(\omega)) = \int_0^{\infty} (u_0(t), E_0(t), f(t))\mathrm{e}^{-i\omega t}\, dt.$$

It can be shown that the gradient of the misfit functional (30) has the form

$$\nabla_{c_{l_2}(z)}\Phi_1[c_{l_2}(z)](s) = -2\,\mathrm{Re}\int_{\omega_1}^{\omega_2}\left[\hat{u}_0(\omega) - \hat{B}_1[c_{l_2}(z)](\omega)\right] \times$$
$$\Big((a'_{11}\overline{G}_{11}(s,\omega) + a'_{21}\overline{G}_{12}(s,\omega))\overline{\hat{u}}(s,\omega) +$$
$$(a'_{12}\overline{G}_{11}(s,\omega) + a'_{22}\overline{G}_{12}(s,\omega))\overline{\hat{v}}(s,\omega)\Big)\, d\omega,$$

$$a'_{11} = -\frac{2\rho_{0,l}}{\rho_0}c_{l_2} - \frac{\rho_{0,s}-\rho_{0,l}}{\rho_0}\tilde{Z}, \quad a'_{12} = 2\frac{\rho_{0,l}}{\rho_0}(c_{l_2}-\tilde{Z}),$$

$$a'_{21} = 2\frac{\rho_{0,s}}{\rho_0}(c_{l_2}-\tilde{Z}), \quad a'_{22} = -\frac{2\rho_{0,s}}{\rho_0}c_{l_2} + \frac{\rho_{0,s}-\rho_{0,l}}{\rho_0}\tilde{Z},$$

$$\tilde{Z} = c_{l_2} + \frac{c_{l_2}^2 - c_{l_1}^2}{\sqrt{\frac{1}{4}(c_{l_1}^2 - c_{l_2}^2)^2 - \frac{16}{9}\frac{\rho_{0,l}\rho_{0,s}}{\rho_0^2}c_t^4}}\frac{c_{l_2}}{2}.$$

Here $G_{ij}(z,\omega)$ is Green's function for the operator $A\frac{d^2}{dz^2} - I\omega^2$, $A = (a_{ij})_{2\times 2}$, $a_{11} = -a_1$, $a_{12} = a_2$, $a_{21} = a_3$, $a_{22} = -a_4$, I is the identity matrix, a bar over the function denotes the complex conjugation.

The gradient of functional (31) is given in work [1], moreover the function $w = -i\omega H(\sigma_s\hat{u} + \sigma_l\hat{v})$ is used as function w belonging to the right-hand side of formula (9) [1].

5. Numerical experiments

A chosen model was discussed in [1] (the distribution of the velocity is shown in Figure 34, and the distribution of the conductivity of a porous elastic body and liquid in Figures 36 and 38). In this case, the sewing conditions at the interfaces of layers were added:

$$[\hat{u}]|_{z=z_k} = [\hat{v}]|_{z=z_k} = [\hat{\hat{h}}_{33} + \hat{p}]|_{z=z_k} = [\frac{\rho_{0,l}}{\rho_0}\hat{p}]|_{z=z_k} = 0,$$

$$[\hat{E}]|_{z=z_k} = [\sigma^{-1}\hat{E}_z]|_{z=z_k} = 0, \quad \omega \in (\omega_1, \omega_2).$$

The initial velocity approximation $c_{l_2}(z)$, shown in Figure 34 by a dashed line, was chosen in the form of a linear function not containing any information about waveguides and high-speed layers. The initial approximations for the conductivity of the liquid and porous elastic body are shown in Figures 36 and 38 respectively. Intensity of electric field $E(t)$ calculated for them is shown in Figure 42 by a dashed line.

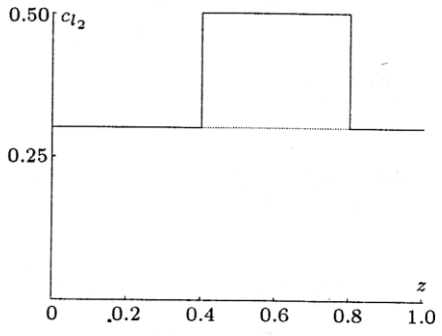

Figure 34

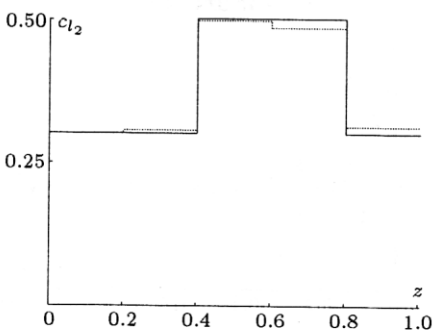

Figure 35

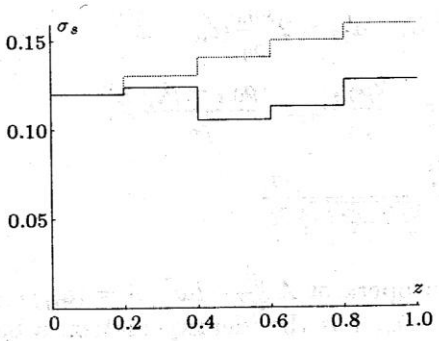

Figure 36

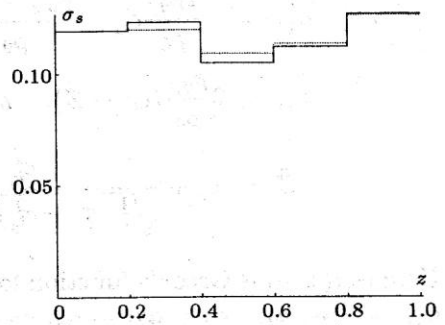

Figure 37

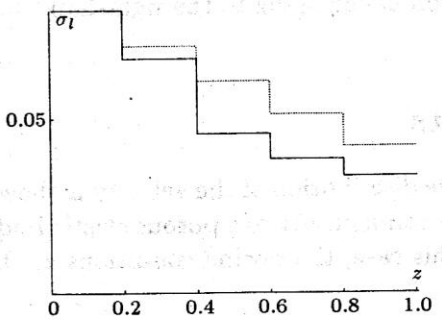

Figure 38

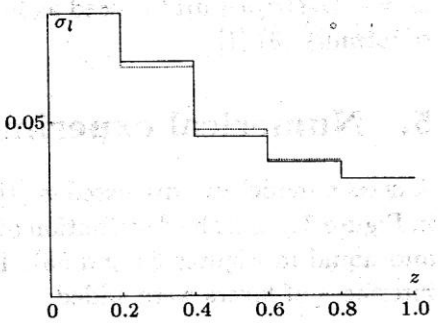

Figure 39

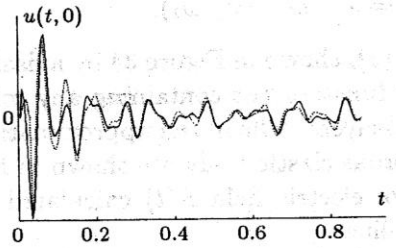

Figure 40

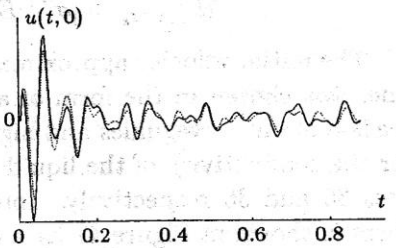

Figure 41

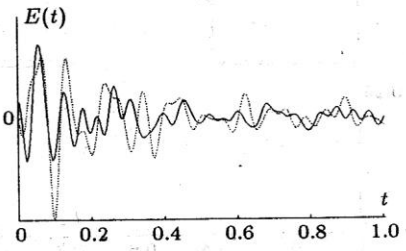

Figure 42

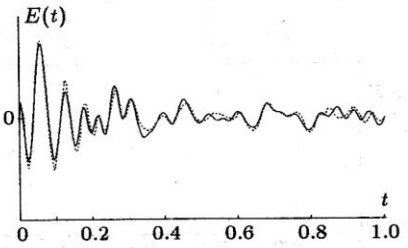

Figure 43

The velocity $c_{l_2}(z)$ was reconstructed at the first stage. The obtained velocities are shown in Figure 35. The wave field $u(t,0)$ on the surface calculated for initial approximation is presented in Figure 40, and for reconstructed approximation is presented in Figure 41.

Then the conductivity of the medium $\sigma(z)$ was reconstructed. Using Archie's law and the determination of conductivity, the conductivities of the liquid (Figure 39) and elastic porous body (Figure 37) were calculated. The electric field intensity on the surface calculated for them is shown in Figure 43.

References

[1] Imomnazarov Kh.Kh. On one class of combined one-dimensional inverse problems for Maxwell's equation and an equation of the continual filtration theory // Proc. of the Institute of Computational Mathematics and Mathematical Geophysics of the Siberian Branch of the Russian Academy of Sciences, Ser. Mathematical Modeling in Geophysics. – Novosibirsk, 1998. – № 5. – P. 61–73 (in Russian).

[2] Imomnazarov Kh.Kh. The uniqueness of one combined one-dimensional inverse problem for Maxwell's equation and an equation of the continual filtration theory // Abstracts of the International Conference "Degenerating and composite type equations", Fergana. – 1998. – P. 40–41 (in Russian).

[3] Imomnazarov Kh.Kh. Combined one-dimensional inverse problems for Maxwell's equations and an equation of the continual filtration theory // Appl. Math. Lett. – 1999. – Vol. 12, № 2. – P. 45–49.

[4] Imomnazarov Kh.Kh. Uniqueness of the solution to combined one-dimensional inverse problems for Maxwell's equations and equations of porous media // Comp. Appl. Math. (to appear).

[5] Dorovsky V.N., Imomnazarov Kh.Kh. A mathematical model for the movement of a conducting liquid through a conducting porous medium // Math. Comput. Modelling. – 1994. – Vol. 20, № 7. – P. 91–97.

[6] Imomnazarov Kh.Kh. Archie's law for a mathematical model of movement of a conducting liquid through a conducting porous medium // Appl. Math. Lett. – 1998. – Vol. 11, № 6. – P. 135–138.

[7] Jackson P.D., Taylor-Smith D., Stanford P.N. Resistivity–porosity–particle shape relationships for marine sands // Geophysics. – 1978. – Vol. 43, № 6. – P. 1250–1268.

[8] Alekseev A.S., Avdeev A.V., Cheverda V.A., Fatianov A.G. Wave processes in vertically inhomogeneous media: a new strategy for a velocity inversion // Inverse Problems. – 1993. – Vol. 9, № 3. – P. 367–390.

[9] Avdeev A.V., Goryunov E.V., Priimenko V.I., Numerical solution to the inverse problem of electromagnetic elasticity // Matematicheskoye Modelirovaniye. – Moscow: Nauka, 1997. – Vol. 9, № 10. – P. 54–66 (in Russian).

[10] Imomnazarov Kh.Kh. Mathematical models of nonlinear geophysical processes in porous elastic body: PhD dissertation. – Novosibirsk: Computing Center, 1995. – P. 88 (in Russian).